

Molecular dynamics simulation of human neurohypophyseal hormone receptors complexed with oxytocin – modeling of an activated state

MAGDALENA J. ŚLUSARZ,* RAFAŁ ŚLUSARZ and JERZY CIARKOWSKI

Faculty of Chemistry, University of Gdańsk, Sobieskiego 18, 80-952 Gdańsk, Poland

Received 5 April 2005; Revised 14 June 2005; Accepted 28 June 2005

Abstract: The neurohypophyseal hormone oxytocin (CYIQNCPLG-NH₂, OT) is involved in the control of labor, secretion of milk and many social and behavioral functions *via* interaction with its receptors (OTR) located in the uterus, mammary glands and peripheral tissues, respectively. In this paper we propose the interactions responsible for OT binding and selectivity to OTR versus vasopressin ([F3,R8]OT, AVP) receptors: V1aR and V2R, all three belonging to the Class A G protein-coupled receptors (GPCRs). Three-dimensional models of the activated receptors were constructed using a multiple sequence alignment and the activated rhodopsin–transducin (MII–Gt) prototype [Ślusarz and Ciarkowski, 2004] as a template. The 1 ns unconstrained molecular dynamics (MD) of three pairs of receptor–OT complexes (two complexes per each receptor) immersed in the fully hydrated 1-palmitoyl-2-oleoyl-*sn*-glycero-3-phosphatidylcholine (POPC) lipid bilayer was conducted in the AMBER 7.0 force field. The relaxed models of ligand–receptor complexes were used to identify the putative binding sites of OT. The stabilizing interactions with conserved Gln residues in all complexes were identified. The nonconserved hydrophobic residues were proposed as responsible for OTR–OT selectivity and ligand recognition. These results provide guidelines for experimental site-directed mutagenesis and if confirmed, they may be helpful in designing new selective OT analogs with both agonistic or antagonistic properties. Copyright © 2005 European Peptide Society and John Wiley & Sons, Ltd.

Keywords: GPCR agonist activation; molecular dynamics; oxytocin; phospholipid bilayer

INTRODUCTION

The neurohypophyseal nonapeptide oxytocin (CYIQNCPLG-NH₂, OT) synthesized in the paraventricular and supraoptic nuclei of the hypothalamus is transported from the magnocellular neurons to the posterior lobe of the pituitary where it is released into the general circulation [1,2]. Partial OT synthesis has been found in the uterus, placenta, corpus luteum, testes and the amnion of various species [3]. OT has a disulfide bridge, which results in an *N*-terminal tocin ring Cys1–Cys6 and a *C*-terminal linear tripeptidic tail. The major physiological function of OT is to induce contractions of uterine smooth muscle and mammary myoepithelium; moreover, OT plays a crucial role in many reproductive, behavioral and social functions [4–9]. OT receptors

(OTR) are found in the membranes of the uterine smooth muscle cells and myoepithelial cells around the milk ducts and alveoli in the mammary glands as well as in other peripheral tissues [5,10–13]. OTR belongs to the Class A G protein-coupled receptor family (GPCR) [14,15] and is included in the neurohypophyseal hormone receptor subgroup, along with the arginine vasopressin ([F3,R8]OT, AVP) receptor subtypes (V1aR, V1bR and V2R respectively) [10,16–18]. The peptide sequences of AVP and OT differ only in the amino acids at positions 3 and 8. Ile in position 3 and Arg in position 8 are crucial for stimulation of OTR and for interaction with vasopressin receptors respectively [19]. The difference in the polarity of these amino acid residues is supposed to enable either hormone to interact with the respective receptors [10]. In Table 1, experimental affinities of OT and AVP toward the respective receptors are given [20].

The largest and best studied Class A of GPCR attains sequence similarity up to 20% within the heptahelical transmembrane domain (7TM) [21] and includes rhodopsin (RD), i.e. the only GPCR with resolved structure on atomic resolution (for inactive 'dark' bovine RD) [22]. It is an agreement regarding 3D-structural homology within 7TM among Class A of GPCR; thus, RD makes a good structural template for other family members [23–28]. GPCRs transduce messages as different as photons, Ca²⁺, odorants, nucleotides, nucleosides, peptides, lipids and proteins

Abbreviations: AVP, arginine vasopressin, vasopressin; CSA, constrained simulated annealing; EL, extracellular loop; G protein, guanine nucleotide-binding protein; GPCR, G protein-coupled receptor; Gq/11, G protein class interacting with phospholipase C; Gs, G protein class interacting with adenylyl cyclase; IL, intracellular loop; MD, molecular dynamics; MII, Meta II, activated form of rhodopsin; OT, oxytocin; OTR, oxytocin receptor; PME, particle-mesh Ewald; POPC, 1-palmitoyl-2-oleoyl-*sn*-glycero-3-phosphatidylcholine; RD, rhodopsin; RMSd, root mean square deviation; TM, transmembrane α -helix; V1aR, vasopressin V1a receptor; V2R, vasopressin V2 receptor; 7TM, heptahelical transmembrane domain.

*Correspondence to: M. J. Ślusarz, Faculty of Chemistry, University of Gdańsk, Sobieskiego 18, 80-952 Gdańsk, Poland; e-mail: magda@chem.univ.gda.pl

Table 1 Experimental affinities of OT and AVP toward respective receptors. The affinity values are given in the IU/mg [20]

	OTR	V1aR	V2R
OT	450	5	5
AVP	17	412	465

[29]. They occupy almost 3% of the human genome [30] and mediate actions of more than 50% of drugs on the market [31,32]. GPCRs are transmembrane proteins consisting of seven hydrophobic transmembrane α -helices (TM) successively connected with alternating extracellular (EL) and intracellular (IL) hydrophilic loops, beginning with an extracellular *N*-terminus and ending with a cytosolic *C*-terminus [22,28,33]. Although the molecular mechanism of GPCR activation is unknown, some of its aspects are generally accepted. In the case of RD, the mechanism of activation involves movement of the TM6, TM7 and TM2 cytosolic halves, with accompanying loop fragments, outside of the 7TM bundle [34,35]. The mentioned dislocation of the cytosolic side of TM6 is additionally accompanied by its clockwise (viewing from the cytosol) rotation [34]. It seems that activation of a GPCR is associated with an allosteric rearrangement in order to open the cavity on the receptor cytosolic side that is capable of accommodating interacting fragments of a guanine nucleotide-binding protein (G protein) at the receptor–G protein interface. The heterotrimeric G protein consists of three subunits, termed α , β and γ [36,37]. It is known that the *C*-terminal peptides Gt_α (340–350) [38,39] and Gt_γ (60–72) farnesyl [40] of the α and γ segments, respectively, independently stabilize activated rhodopsin (Meta II, MII) [41–43]. The Gt_α *C*-terminal fragment makes an α -helical extension of the last $\alpha 5$ helix, potentially fitting into the MII cavity on its cytosolic side [44–46]. Thus, it was proposed that in any receptor–G protein system, an agonist-induced rearrangement occurs, involving conservative residues of both parties in a set of consensus interactions [46]. The low-resolution model of the MII monomer, which had Gt_α (338–350) docked was used in this study as the template for construction of three-dimensional models of activated neurohypophyseal hormone receptors – OTR, V1aR and V2R. OTR and V1aR are functionally coupled to the Gq/11 protein that stimulates the activity of phospholipase C, whereas V2R stimulates the Gs protein, resulting in the activation of adenylyl cyclase [6,12]. The models of OTR, V1aR and V2R, respectively, along with suitable interacting G_α fragments were used to determine the OT binding site, as described in the following text.

MATERIALS AND METHODS

Parameterization and Building of the Receptor– G_α –OT Models

Nonstandard amino acid residues and other structure fragments were parameterized as recommended in the AMBER 7.0 manual [47]. Specifically, the point atom charges were fitted by applying the RESP procedure [48,49] to the electrostatic potential calculated in the 6–31G* basis set using the program GAMESS [50].

The three-dimensional model of OT was built using the coordinates of pressinoic acid [51] and the BIOPOLYMER module of the SYBYL package [52].

The three-dimensional models of activated neurohypophyseal hormone receptors (OTR, V1aR and V2R) were built by (i) applying a multiple sequence alignment [53] for RD, OTR, V1aR and V2R, respectively (Figure 1) and subsequently (ii) using the previously described 3D model of MII– Gt_α (338–350), which is the appropriate modification of the X-ray RD structure [46] as the template. The computer mutations, insertions and/or deletions necessary to obtain proper receptor amino acid sequences were done using standard AMBER 7.0 tools [47] and the BIOPOLYMER module of SYBYL [52]. Specifically, the transmembrane RD residues were replaced with the equivalent residues from the respective human neurohypophyseal hormone receptor essentially on a one-to-one basis (for specific residue substitutions see sequence alignment, Figure 1). Missing extra- and intracellular loops as well as the *N*- and the *C*-termini were added using the homology modeling/loop closure tool(s) again as implemented in the SYBYL's BIOPOLYMER module [52]. The putative conservative disulfide, coupling EL1 with EL2 [54], was set manually, resulting in the Cys112–Cys192, Cys124–Cys203 and Cys112–Cys187 links in V2R, V1aR and OTR, respectively. The *C*-terminal fragments of appropriate G-proteins necessary to keep receptors in an activated state were modeled using the known structures of the G_α subunits of Gq/11 and Gs proteins (UniProt entries: O15975 for Gq/11 and P63092 for Gs) [55]. The *C*-terminal peptides were manually docked into the receptor cavities analogous to the cavity that binds Gt_α (340–350) in the MII structure. Subsequently, the systems were energy-minimized and relaxed using the AMBER 7.0 force field [47]. The relaxed OTR model presented in Figure 2 is superimposed with the structure of an inactive OTR (modeled on the inactive RD template and used in our former studies [56–59]).

Docking and MD Simulation

In the next step, OT was docked to the OTR–Gq/11(347–359), V1aR–Gq/11(347–359) and V2R–Gs(382–394) systems, using a modified genetic algorithm as implemented in the AutoDock program [61,62]; details of the docking procedure were described elsewhere [56,57,63]. Briefly, the populations of 3×150 complexes were generated. Relaxation of the complexes using a constrained simulated annealing (CSA) protocol *in vacuo* for 15 ps [64,65], followed by energy minimization, with positional constraints on C^α atoms in transmembrane domain in order to maintain the receptors shape in homology to MII was carried out. The two lowest-energy systems per each OTR–Gq/11(347–359)–OT, V1a–Gq/11(347–359)–OT and V2–Gs(382–394)–OT complexes were chosen. Subsequently, these six selected complexes were inserted into the

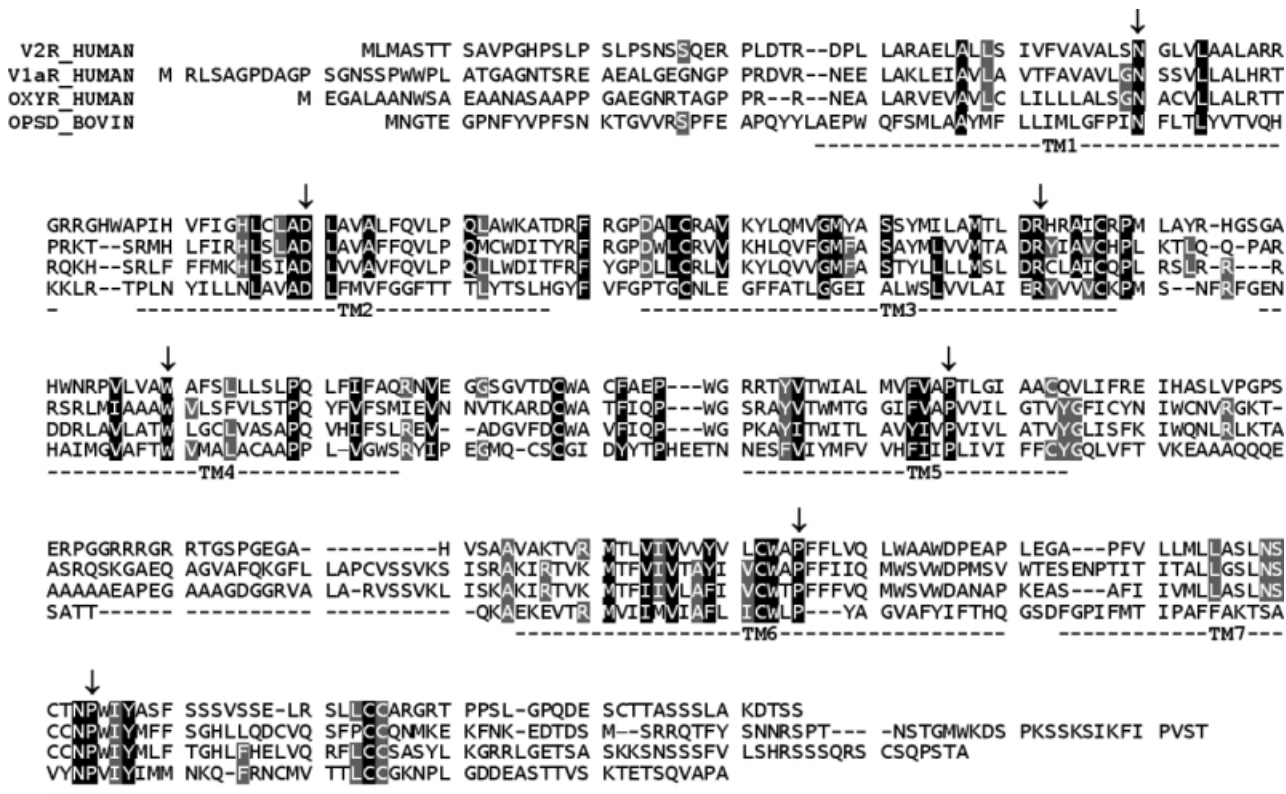


Figure 1 Primary sequence alignment of the human neurohypophyseal hormone receptors (OTR, V1aR and V2R), and bovine rhodopsin, done using the Multalin program [53]. The putative transmembrane helices 1–7 are underlined. The conservative residues, indicative of high-level similarity within the subfamily, are shown in black while those with lower-level similarity are shown in gray [5]. The 'N50 residues are marked with an arrow [60]. As a result of not higher than 20% sequential homology among class A GPCR, the mutations of residues in 7TM that are necessary to convert RD into OTR/V1aR/V2R reached 82/80/85%, or 165/165/172 residues, respectively.

1-palmitoyl-2-oleoyl-*sn*-glycero-3-phosphatidylcholine (POPC) membrane model [66,67] and submitted to the MD simulation carried out in AMBER 7.0 force field [47], using particle-mesh Ewald (PME) electrostatic summation [68–70]. The periodic box of each complex consisted of 120 POPC lipid molecules in two layers, about 3500 water molecules (slightly varying in number, depending on the shape of individual receptors), and Cl⁻ counterions (to neutralize the charge of the complexes). For all components of complexes, the OPLS [71] united atom parameters were applied. The flat-bottom soft harmonic-wall restraints were imposed onto the φ , ψ and ω peptide angles of the 7TM amino acid residues to avoid unfolding or any other unwanted modifications of the TM helices. In accordance with the standard AMBER protocol, the positional TM C α constraints were used exclusively for the first 100 ps of the simulation while heating the system from 0 to 300 K, to prevent the helices from deformation at the initial steps of MD due to heavy gradients at these steps. Finally, the energy minimization of the 1 ns MD snapshots in AMBER 7.0 force field [47] was done.

RESULTS

After MD simulation six relaxed receptor-G α -segment-OT complexes were obtained. One complex per

receptor, that of lower energy in any pair, was finally selected for further detailed examination. The OT residues are identified using three-letter codes with the indices in parentheses, e.g. Tyr(2), while the receptor residues are identified using one-letter codes with the universal Class A indices [60] placed as superscripts, followed by the absolute numbers, e.g. OTR V7^{.38}314 or by absolute numbers of respective (OTR, V1aR, V2R) receptor residues, e.g. Q^{2.61}(96, 108, 96) describing the interactions of conservative residues. Residues placed in loops are identified with one-letter codes, followed only by the residue absolute number, e.g. EL2 E198.

According to this universal notation, the most conserved residue in the TM helix 'N' is designated as a reference 'N.50'. Receptor amino acid residues interacting with the ligand were identified using the distance criteria. Thus, all amino acid residues where an atom was not farther than 3.5 Å from any atom of OT residues was considered as interacting with the latter. Amino acid residues meeting these criteria are listed in Table 2. The most essential interactions between OT and the receptors (OTR, V1aR and V2R, respectively) were characterized by visual inspection and they are presented in Figure 3.

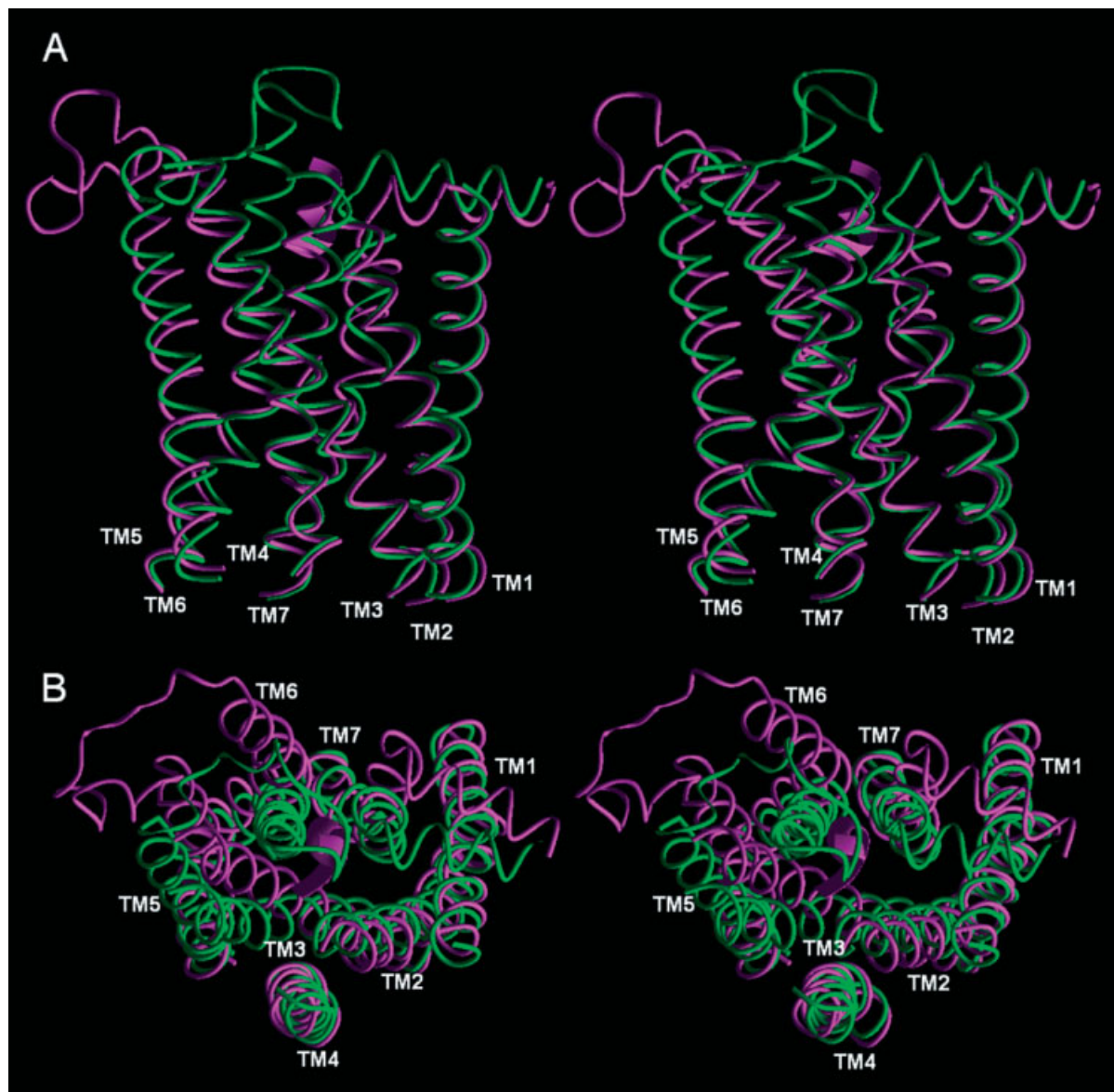


Figure 2 Stereodiagrams of the activated OTR model (magenta) superimposed on the structure of inactive OTR (green). Panel A – side view, parallel to the cell membrane; panel B – a view from the cytosolic side. The TM helices are marked. The C-terminal segment of the $G_t\alpha$ subunit is presented as a ribbon. Both N- and C-termini as well as the loops, except of the IL3 are omitted for clarity.

Conserved Polar Residues are Responsible for OT Binding to Neurohypophysial Hormone Receptors

The highly conserved (see sequence alignment, Figure 1) receptor residues, $Q^{2.57}$ (92, 104, 92 for OTR, V1aR, V2R, respectively), $Q^{2.61}$ (96, 108, -), $Q^{3.32}$ (119, 131, 119), $V^{3.28}$ (115, 127, -), $K^{3.29}$ (116, 128, -), $M^{3.36}$ (123, 135, 123), $Q^{4.60}$ (171, 185, -), $F^{6.51}$ (291, 307, 287), $Q^{6.55}$ (295, 311, 291) $L^{7.40}$ (316, 335, -) and $S^{7.43}$ (319, 338, -), participate in the binding of OT to all three investigated receptors or occur only in complexes of OT with OTR and V1aR, but not V2R (Table 2 and Figure 3). Therefore, Gln residues appear to be especially important anchors keeping OT in active conformation as well as in proper location inside the

binding site of the receptor. In the OTR–OT complex, two Gln residues, $Q^{2.57}$ 92 and $Q^{6.55}$ 295, seem to be most important for OT binding because they can interact with more than one OT residue simultaneously (Figure 3). The $Q^{2.57}$ 92 is mainly interesting due to strong, double interaction with the N-terminal tocin ring of OT. The carboxamide of $Q^{2.57}$ 92 may simultaneously form two hydrogen bonds with the amino group of Cys(1) and with the hydroxyl group of Tyr(2) in OT. The $Q^{6.55}$ 295 is also important because of its interaction with Ile(3). There is a hydrogen bond formed between the carboxamide of $Q^{6.55}$ 295 and the main chain carbonyl of Ile(3), whereas the aliphatic side chain of $Q^{6.55}$ 295 may interact with OT Leu(8).

Table 2 List of the OTR, V1aR and V2R residues, involved in the interactions with OT

TM 'N'domain	OTR	V1aR	V2R	Universal numbering ^a
TM1	E42	E54	—	1.35
TM2	V88	V100	—	2.53
	Q92	Q104	Q92	2.57
	Q96	Q108	—	2.61
TM3	V115	V127	—	3.28
	K116	K128	—	3.29
	Q119	Q131	Q119	3.32
	V120	V132	M120	3.33
	M123	M135	M123	3.36
	F124	—	Y124	3.37
TM4	A167	L181	L170	4.56
	—	S182	—	4.57
	Q171	Q185	—	4.60
	S176	—	—	4.65
	L177	M191	Q180	4.66
TM5	—	—	R203	5.36
	—	Y216	—	5.38
	—	V217	V206	5.39
	I204	M220	I209	5.42
	—	—	A210	5.43
TM6	Y209	F225	F214	5.47
	P290	—	—	6.50
	F291	F307	F287	6.51
	V294	—	—	6.54
	Q295	Q311	Q291	6.55
	V299	V315	A295	6.59
TM7	—	—	P298	6.62
	F311	I330	F307	7.35
	V314	—	—	7.38
	M315	A334	M311	7.39
	L316	L335	—	7.40
	A318	—	—	7.42
	S319	S338	—	7.43
N321	—	—	7.45	
EL2	R178	I192	R181	
	F185	K199	T190	
	F191	R201	G201	

^a Ref. 60.

In the complexes of OT with the vasopressin V1a and V2 receptors, the equivalent Q^{6.55} (311 and 291 respectively) could also strongly interact with OT. In the V1aR–OT complex, the hydrogen bond could be formed between the carboxamide of Q^{6.55}311 and the main chain carbonyl of Asn(5). In the complex with V2R, there is a possibility of hydrogen bonding between the carboxamide of Q^{6.55}291 and the amino group of OT Cys(1). Furthermore, in this complex two hydrogen bonds between Gly(9) carbonyl and/or the Q^{2.57}92 and Q^{3.32}119 carboxamides could be observed.

The remaining conserved residues (Table 2): V^{3.28} (115, 127, –), M^{3.36} (123, 135, 123), F^{6.51} (291, 307, 287), L^{7.40} (316, 335, –) and S^{7.43} (319, 338, –), hydrophobic in nature, are also essential for OT binding; however, not as important as described above are the hydrophilic Gln residues that form the putative binding pocket for OT.

The highly conserved N^{7.45}321 appears only in the OTR–OT complex. There is a possibility of forming a hydrogen bond between the carboxamide of N^{7.45}321 and the amino group of OT Cys(1). All interactions with the Cys(1) amino group have been considered less important for OT binding, because it is known that deletion of *N*-terminal amine of OT does not decrease the agonistic properties [72,73].

Specific Hydrophobic Interactions are Responsible for Selective Binding of OT to OTR

In the OTR–OT complex, there are several strong interactions between hydrophobic OTR residues and OT Ile(3) and Leu(8) (Figure 3, panels A and B). It has been experimentally proven that substitutions in position 8 of OT do not cause significant changes in affinity toward OTR, but the replacement of Ile(3) with other amino acid residues causes significant decrease of this affinity [19]. Therefore, the interactions involving Ile(3), identified in this work, might determine selectivity of binding of OT to OTR. The interactions involving Leu(8) were also perceived as very important for OT binding, but not critical for selectivity of this binding. The following OTR residues: L^{4.66}177, I^{5.42}204, Y^{5.47}209, and V^{6.59}299 interact with Leu(8). Although, all of them are nonconserved ones (Figure 1), nonetheless the equivalent residues also in V1aR and V2R interact with OT (Table 2). Thus, we believe they are not as important as residues exclusively interacting with Ile(3) in the OTR–OT complex.

The latter are the hydrophobic OTR residues: P^{6.50}290, V^{6.54}294, V^{7.38}314 and A^{7.42}318. The strongest interactions involve V^{6.54}294 and V^{7.38}314, both non-conserved ones (Figure 1), whose side chains are situated very close to the side chain of the OT Ile(3) (Figure 3). It is significant that all the four residues, P^{6.50}290, V^{6.54}294, V^{7.38}314 and A^{7.42}318, interact with OT Ile(3) exclusively in OTR and, in addition both strong interacting residues (V^{6.54}294 and V^{7.38}314) are non-conserved ones. Thus, we think they are mainly responsible for selectivity of binding of OT to OTR.

Moreover, the nonconserved S^{4.65}176 seems to be also important for OT binding. There is a possibility of a hydrogen bonding between hydroxyl group of S^{4.65}176 and the carbonyl group of Gly(9). This interaction could occur exclusively in the complex of OT with OTR and thus may be also responsible for selectivity.

In addition to residues situated in the transmembrane regions, residues located in the extracellular domain (EL2) also interact with OT. There is

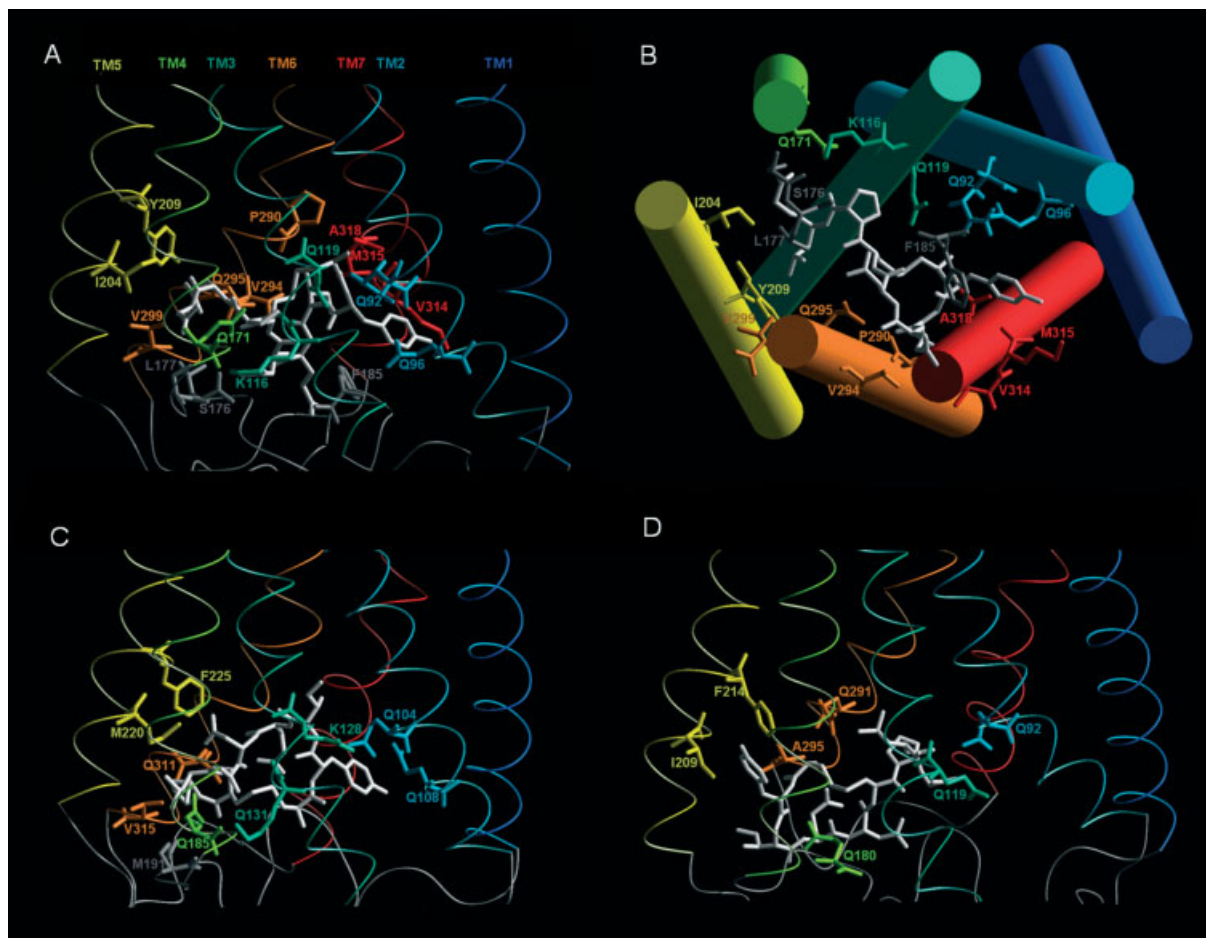


Figure 3 Representation of the OT-binding pocket in neurohypophyseal hormone receptors. Panel A and B – OTR, panel C – V1aR, panel D – V2R. Only the extracellular halves of the receptors are shown, extracellular side is at the bottom in panels A, C and D. The TM helices are colored from blue (TM1) to red (TM7), and are marked in panel A. The N-terminus and the extracellular loops: EL1 and EL2 are omitted for clarity. The binding amino acid residues are marked and their side chains exposed; they are colored in harmony with TM colors while the EL2 residues are gray.

a strong aromatic–aromatic interaction between the phenyl rings of Tyr(2) and EL2 F185. This interaction is also exclusive for the OTR–OT complex and thus may be accordingly crucial for selectivity of binding of OT to OTR.

DISCUSSION

In this work, the low-resolution model of MII–Gt_α (338–350) is for the first time used as the template for building the models of activated neurohypophyseal hormone receptors. In our previous works, concerning OT and vasopressin antagonists, we used the receptor models in inactive states [56–59]. Available force fields are not advanced enough to span timescales as long as those typical of an agonist-induced activation of a receptor. Hence, we decided to use the prototype of the activated form of RD [46] as the template of activated receptor models. These models subsequently served us for MD simulation and analysis of receptor–agonist

interactions. The model of activated OTR used in this work, superimposed with the model of inactive OTR used in our former studies [56,58,59] is shown in Figure 2.

The justification of the active RD model has already been discussed [46]. The current MD of receptor–OT complexes did not lead to significant conformational changes of the receptor structures, and the root mean square deviations (RMSd) measured on the C^α carbons of the 7TM were 2.27 Å for OTR, 2.12 Å for V1aR and 3.52 Å for V2R. The higher RMSd for V2R in our opinion results from lack of important receptor–ligand interactions with conserved polar residues (see the *Results* section and experimental affinities in Table 1). On the contrary, in OTR and to a lower degree in V1aR, there are a great number of TM2–TM7 residues, which, due to their interaction with OT, prevent from extensive displacements of the helices to which they belong. Thus, OTR and V1aR would get better stabilized in their active conformations than V2R. Indeed, the location of the ligand is somewhat different in V2R than in

OTR and V1aR (see the following text and Figure 3). Thus, in all complexes OT is buried in a binding pocket of the receptors, extending from the extracellular domain into ~ 15 Å depth of the transmembrane region (Figure 3, panels A, C and D). The location of OT is rather horizontal (perpendicular to longer axis of the receptor) in all complexes contrary to OT antagonists, as described in our previous papers [58,59]. In the complexes of OT with OTR and V1aR, the tocin ring is located within TM1, TM2 and TM7 domains, whereas the C-terminal tail is situated close to TM4 and TM5. In V2R–OT complex, the orientation of the ligand is exactly opposite. Therefore, the same highly conserved receptor residues interact with different OT residues in OTR and V1aR than V2R, as described above.

Our results show the probable contribution of the highly conserved Gln residues for binding of OT to all investigated neurohypophyseal hormone receptors. It is significant that all Gln residues, Q^{2.57}, Q^{2.61}, Q^{3.32}, Q^{4.60}, Q^{6.55} and also K^{3.29}, proposed in this work to be involved in OT binding, have been identified as responsible for binding neurohypophyseal hormones and their analogs to rat V1aR by mutagenesis studies [74]. A relatively large number of these interacting residues capable of forming many hydrogen bonds favors the hypothesis that the hormone–receptor complex is stabilized by the network of many interactions, rather than by a few precisely given points of contact [10]. Thus, the Gln residues are not responsible for selectivity, but merely impose location of OT inside the binding domain and keep the ligand in active conformation by forming a network of hydrogen bonds. The lack of some of these stabilizing residues in the V2R–OT complex allows the ligand to dislocate toward the extracellular side during MD (Figure 3). It seems obvious enough that the conserved residues (Table 2 and the *Results* section), both polar and nonpolar, interacting with OT in all three investigated complexes, would rather not pertain to selectivity of binding. However, we observe that the number of these types of interactions is greater in the complex with OTR, than with V1aR and even fewer with V2R, where in the latter some of them do not appear at all. This observation is in agreement with common knowledge about affinity of OT toward neurohypophyseal hormone receptors and it confirms weaker binding of OT to V1aR and V2R – with approximately 400-fold lower affinity than AVP [19,75,76]; Table 1. Moreover, some of residues proposed in this work as responsible for receptor–ligand selectivity, were earlier found as the residues forming the OT binding site [5,77].

The essence of our results is that the nonconserved hydrophobic OTR residues V^{6.54}294 and V^{7.38}314 interacting with OT Ile(3) might be mainly responsible for selectivity of binding of OT to OTR. The EL2 F185 and S^{4.65}176, more exposed to the extracellular side, might also play a significant role in OTR–OT selectivity,

perhaps in recognition of the ligand. The remaining hydrophobic amino acid residues are probably less involved in selectivity, as we have already discussed.

In conclusion, the results presented in this paper provide guidelines for experimental site-directed mutagenesis and if confirmed, they may be helpful in the designing of new selective OTR analogs with antagonistic properties. The latter are widely used in the treatment of preterm labor and dysmenorrhea [78], but in view of the fact that in recent years the OT receptor system has been identified in many different tissues of both sexes. OT analogs could potentially find application in the treatment of many, especially psychiatric, illnesses [5].

Acknowledgements

This work is supported by The Polish Scientific Research Committee (KBN), grant no. 3 T09A 11628, The Ministry of Scientific Research and Information Technology (MNI, Poland) grant no. DS/8372-4-0138-5 and grant for scientific project no. BW/8000-5-0260-5, University of Gdańsk. The computational time in the Academic Computer Center in Gdansk CITASK, Poland, and the Interdisciplinary Center for Mathematical Modeling (ICM) in Warsaw, Poland, is acknowledged.

REFERENCES

1. Brownstein MJ, Russell JT, Gainer HT. Synthesis, transport, and release of posterior pituitary hormones. *Science* 1980; **207**: 373–378.
2. Zimmerman EA, Defendini R. Hypothalamic pathways containing oxytocin, vasopressin, and associated neurophysins. In *International Conference on the Neurohypophysis*, Moses AM, Share L (eds). Karger: New York, 1977; 22–29.
3. Gainer H, Wray S. Cellular and molecular biology of oxytocin and vasopressin. In *The Physiology of Reproduction*, Knobil E, Neill JD (eds). Raven Press: New York, 1994; 1113–1114.
4. Fuchs AR, Fuchs F, Husslein P, Soloff MS, Fernstrom MJ. Oxytocin receptors and human parturition: a dual role for oxytocin in initiation of labor. *Science* 1982; **215**: 1396–1398.
5. Gimpl G, Fahrenholz F. The oxytocin receptor system: structure, function, and regulation. *Physiol. Rev.* 2001; **81**: 629–683.
6. Barberis C, Tribollet E. Vasopressin and oxytocin receptors in the central nervous system. *Crit. Rev. Neurobiol.* 1996; **10**: 119–154.
7. Argiolas A, Gessa GL. Central functions of oxytocin. *Neurosci. Biobehav. Rev.* 1991; **15**: 217–231.
8. Bielsky IF, Young LJ. Oxytocin, vasopressin, and social recognition in mammals. *Peptides* 2004; **25**: 1565–1574.
9. Carter CS. Oxytocin and sexual behavior. *Neurosci. Biobehav. Rev.* 1992; **16**: 131–144.
10. Barberis C, Mouillac B, Durroux T. Structural bases of vasopressin/oxytocin receptor function. *J. Endocrinol.* 1998; **156**: 223–229.
11. Ivell R, Bathgate R, Kimura T, Parry L. Molecular biology of the oxytocin receptor: a comparative approach. *Biochem. Soc. Trans.* 1997; **25**: 1058–1066.
12. Zingg HH. Vasopressin and oxytocin receptors. *Baillieres Clin. Endocrinol. Metab.* 1996; **10**: 75–96.
13. Kimura T. Investigation of the oxytocin receptor at the molecular level. *Adv. Exp. Med. Biol.* 1995; **395**: 259–268.

14. Kimura T, Tanizawa O, Mori K, Brownstein MJ, Okayama H. Structure and expression of a human oxytocin receptor. *Nature* 1992; **356**: 526–529.
15. Kimura T, Ivell R. The oxytocin receptor. *Results Prob. Cell Differ.* 1999; **26**: 135–168.
16. Thibonnier M, Auzan C, Madhun Z, Wilkins P, Berti-Mattera L, Clauser E. Molecular cloning, sequencing, and functional expression of a cDNA encoding the human V1a vasopressin receptor. *J. Biol. Chem.* 1994; **269**: 3304–3310.
17. Birnbaumer M, Seibold A, Gilbert S, Ishido M, Barberis C, Antaramian A, Brabet P, Rosenthal W. Molecular cloning of the receptor for human antidiuretic hormone. *Nature* 1992; **357**: 333–335.
18. Sugimoto T, Saito M, Mochizuki S, Watanabe Y, Hashimoto S, Kawashima H. Molecular cloning and functional expression of a cDNA encoding the human V1b vasopressin receptor. *J. Biol. Chem.* 1994; **269**: 27088–27092.
19. Postina R, Kojro E, Fahrenholz F. Separate agonist and peptide antagonist binding sites of the oxytocin receptor defined by their transfer into the V2 vasopressin receptor. *J. Biol. Chem.* 1996; **271**: 31593–31601.
20. Lebl M, Jošt K, Brtník F. Tables of analogs. In *Handbook of Neurohypophyseal Hormone Analogs*, Jošt K, Lebl M, Brtník F (eds). Vol. 1, Part 2, CRC Press: Boca Raton, 1987; 127–267.
21. Hakak Y, Shrestha D, Goegel MC, Behan DP, Chalmers DT. Global analysis of G protein-coupled receptor signaling in human tissues. *FEBS Lett.* 2003; **550**: 11–17.
22. Palczewski K, Kumasaka T, Hori T, Behnke CA, Motoshima H, Fox BA, Le Trong I, Teller DC, Okada T, Stenkamp RE, Yamamoto M, Miyamoto M. Crystal structure of rhodopsin: a G protein-coupled receptor. *Science* 2000; **289**: 739–745.
23. Sakmar TP. Structure of rhodopsin and the superfamily of seven-helical receptors: the same and not the same. *Curr. Opin. Cell Biol.* 2002; **14**: 189–195.
24. Mirzadegan T, Benko G, Filipek S, Palczewski K. Sequence analyses of G-protein-coupled receptors: similarities to rhodopsin. *Biochemistry* 2003; **42**: 2759–2767.
25. Dowell SJ, Brown AJ. Yeast assays for G-protein-coupled receptors. *Recept. Channels* 2002; **8**: 343–352.
26. Meng EC, Bourne H. Receptor activation: what does the rhodopsin structure tell us? *TIPS* 2001; **22**: 587–593.
27. Hunyady L, Vauquelin G, Vanderheyden P. Agonist induction and conformational selection during activation of a G-protein-coupled receptor. *TIPS* 2003; **24**: 81–86.
28. Ballesteros JA, Shi L, Javitch JA. Structural mimicry in G protein-coupled receptors: implications of the high-resolution structure of rhodopsin for structure-function analysis of rhodopsin-like receptors. *Mol. Pharmacol.* 2001; **60**: 1–19.
29. Bockaert J, Pin JP. Molecular tinkering of G protein-coupled receptors: an evolutionary success. *EMBO J.* 1999; **18**: 1723–1729.
30. Klabunde T, Hessler G. Drug design strategies for targeting G-protein coupled receptors. *ChemBiochem* 2002; **3**: 928–944.
31. Sautel M, Milligan G. Molecular manipulation of G-protein-coupled receptors: a new avenue into drug discovery. *Curr. Med. Chem.* 2000; **7**: 889–896.
32. Becker OM, Shacham S, Marantz Y, Noiman S. Modeling the 3D structure of GPCRs: advances and application to drug discovery. *Curr. Opin. Drug. Discov. Devel.* 2003; **6**: 353–361.
33. Lu Z-L, Saldanha JW, Hulme EC. Seven-transmembrane receptors: crystals clarify. *TIPS* 2002; **23**: 140–146.
34. Hubbell WL, Altenbach C, Hubbell CM, Khorana HG. Rhodopsin structure, dynamics, and activation: a perspective from crystallography, site-directed spin labeling, sulfhydryl reactivity, and disulfide cross-linking. *Adv. Prot. Chem.* 2003; **63**: 243–290.
35. Farrens DL, Altenbach C, Yang K, Hubbell WL, Khorana HG. Requirement of rigid-body motion of transmembrane helices for light activation of rhodopsin. *Science* 1996; **274**: 768–770.
36. Lambright DG, Sondek J, Bohm A, Skiba NP, Hamm HE, Sigler PB. The 2.0 Å crystal structure of a heterotrimeric G protein. *Nature* 1996; **379**: 311–319.
37. Bourne HR. How receptors talk to trimeric G proteins. *Curr. Opin. Cell Biol.* 1997; **9**: 134–142.
38. Koenig BW. Structure and orientation of ligands bound to membrane proteins are reflected by residual dipolar couplings in solution NMR measurements. *ChemBiochem* 2002; **3**: 975–980.
39. Kisselev OG, Kao J, Ponder JW, Fann YC, Gautam N, Marshall GR. Light-activated rhodopsin induces structural binding motif in G protein alpha subunit. *Proc. Natl. Acad. Sci.* 1998; **95**: 4270–4275.
40. Kisselev OG, Downs MA. Rhodopsin controls a conformational switch on the transducin gamma subunit. *Structure* 2003; **11**: 367–373.
41. Hamm HE, Deretic D, Arendt A, Hargrave PA, König B, Hoffman KP. Site of G protein binding to rhodopsin mapped with synthetic peptides from the alpha subunit. *Science* 1988; **241**: 832–835.
42. Martin EL, Rens-Domiano S, Schatz PJ, Hamm HE. Potent peptide analogues of a G protein receptor-binding region obtained with a combinatorial library. *J. Biol. Chem.* 1996; **271**: 361–366.
43. Aris L, Gilchrist A, Rens-Domiano S, Meyer C, Schatz PJ, Dratz EA, Hamm HE. Structural requirements for the stabilization of metarhodopsin II by the C terminus of the alpha subunit of transducin. *J. Biol. Chem.* 2001; **276**: 2333–2339.
44. Janz JM, Farrens DL. Rhodopsin activation exposes a key hydrophobic binding site for the transducin alpha-subunit C terminus. *J. Biol. Chem.* 2004; **279**: 29767–29773.
45. Koenig BW, Kontaxis G, Mitchell DC, Louis JM, Litman BJ, Bax A. Structure and orientation of a G protein fragment in the receptor bound state from residual dipolar couplings. *J. Mol. Biol.* 2002; **322**: 441–461.
46. Ślusarz R, Ciarkowski J. Interaction of class A G protein-coupled receptors with G proteins. *Acta Bioch. Pol.* 2004; **51**: 129–136.
47. Case DA, Pearlman DA, Caldwell JW, Cheatham TE, Wang J, Ross WS, Simmerling CL, Darden TA, Merz KM, Stanton RV, Cheng A, Vincent JJ, Crowley M, Tsui V, Gohlke H, Radmer R, Duan Y, Pitera J, Massova I, Seibel GL, Singh UC, Weiner P, Kollman PA. *Amber 7*. University of California: San Francisco, 2002.
48. Cieplak P, Cornell WD, Bayly C, Kollman PA. Application of the multimolecule and multiconformation RESP methodology to biopolymers: charge derivation for DNA, RNA, and proteins. *J. Comp. Chem.* 1995; **16**: 1357–1377.
49. Bayly CI, Cieplak P, Cornell WD, Kollman PA. A well-behaved electrostatic potential based method using charge restraints for deriving atomic charges: the RESP model. *J. Phys. Chem.* 1993; **97**: 10269–10280.
50. Schmidt MW, Baldrige KK, Boatz JA, Elbert ST, Gordon MS, Jensen JH, Koseki S, Matsunaga N, Nguyen KA, Su S, Windus TL, Dupuis M, Montgomery JA. The general atomic and molecular electronic structure system. *J. Comput. Chem.* 1993; **14**: 1347–1363.
51. Langs DA, Smith GD, Stezowski JJ, Hughes RE. Structure of pressinoic acid: the cyclic moiety of vasopressin. *Science* 1986; **232**: 1240–1242.
52. *Sybyl*® 6.8. Tripos Inc.; St. Louis, USA.
53. Corpet F. Multiple sequence alignment with hierarchical clustering. *Nucleic Acids Res.* 1998; **16**: 10881–10890.
54. Iismaa TP, Biden TJ, Shine J. Chapter 1. *G Protein-Coupled Receptors*. Springer-Verlag: Heidelberg, 1995; 16–22.
55. Apweiler R, Bairoch A, Wu CH, Barker WC, Boeckmann B, Ferro S, Gasteiger E, Huang H, Lopez R, Magrane M, Martin MJ, Natale DA, O'Donovan C, Redaschi N, Yeh LS. UniProt: the universal protein knowledge base. *Nucleic Acids Res.* 2004; **32**: 115–119.
56. Ślusarz M, Ślusarz R, Kaźmierkiewicz R, Trojnar J, Wiśniewski K, Ciarkowski J. Molecular modeling of the neurohypophyseal receptor/atosiban complexes. *Protein Pept. Lett.* 2003; **10**: 295–302.

57. Ślusarz R, Ślusarz MJ, Kaźmierkiewicz R, Lammek B. Molecular modeling of interaction of the vasopressin analogs with vasopressin and oxytocin receptors. *QSAR Comb. Sci.* 2003; **22**: 865–872.
58. Ślusarz MJ, Ślusarz R, Meadows R, Trojnar J, Ciarkowski J. Molecular dynamics of complexes of atosiban with neurohypophyseal receptors in the fully hydrated phospholipid bilayer. *QSAR Comb. Sci.* 2004; **23**: 536–545.
59. Ślusarz MJ, Gieldoń A, Ślusarz R, Meadows R, Trojnar J, Ciarkowski J. Study of new oxytocin antagonist barusiban (Fe200 440) affinity toward human oxytocin receptor versus vasopressin V1a and V2 receptors – molecular dynamics simulation in POPC bilayer. *QSAR Comb. Sci.* 2005; **24**: 603–610.
60. Ballesteros JA, Weinstein H. Integrated methods for modeling G-protein coupled receptors. *Methods Neurosci.* 1995; **25**: 366–428.
61. Morris GM, Goodsell DS, Halliday RS, Huey R, Hart WE, Belew RK, Olson AJ. Automated docking using a Lamarckian genetic algorithm and empirical binding free energy function. *J. Comput. Chem.* 1998; **19**: 1639–1662.
62. Solis FJ, Wets JB. Minimization by random search techniques. *Math. Oper. Res.* 1981; **6**: 19–30.
63. Goodsell DS, Morris GM, Olson AJ. Docking of flexible ligands: applications of AutoDock. *J. Mol. Recognit.* 1996; **9**: 1–5.
64. Kirkpatrick S, Gelatt CD Jr, Vecchi MP. Optimization by simulated annealing. *Science* 1983; **220**: 671–680.
65. Clore GM, Nilges M, Brünger AT, Karplus M, Gronenborn AM. A comparison of the restrained molecular dynamics and distance geometry methods for determining three-dimensional structures of proteins on the basis of interproton distance restraints. *FEBS Lett.* 1987; **213**: 269–277.
66. Murzyn K, Róg T, Jezierski G, Takaoka Y, Pasenkiewicz-Gierula M. Effects of phospholipid unsaturation on the membrane/water interface: a molecular simulation study. *Biophys. J.* 2001; **81**: 170–183.
67. Pasenkiewicz-Gierula M, Murzyn K, Róg T, Czaplowski C. Molecular dynamics simulation studies of lipid bilayer systems. *Acta Biochim. Pol.* 2000; **47**: 601–611.
68. Ewald PP. Die berechnung optischer und elektrostatischer gitterpotentiale. *Ann. Phys.* 1921; **64**: 253–287.
69. Darden T, York D, Petersen L. Partial mesh ewald: an $N \times \log(N)$ method for ewalds sums in large systems. *J. Chem. Phys.* 1993; **98**: 10 089–10 092.
70. Essmann UL, Perera ML, Berkowitz T, Darden T, Lee H, Pedersen LG. A smooth particle mesh ewald method. *J. Chem. Phys.* 1995; **103**: 8577–8593.
71. Jorgensen WL, Tirado-Rives J. The OPLS potential functions for proteins. Energy minimization for crystals of cyclic peptides and crambin. *J. Am. Chem. Soc.* 1988; **110**: 1657–1666.
72. Sawyer WH, Grzonka Z, Manning M. Neurohypophyseal peptides. Design of tissue-specific agonists and antagonists. *Mol. Cell Endocrinol.* 1981; **22**: 117–134.
73. Hope DB, Walti M. (1-(1-2-Hydroxy-3-mercaptopropanoic acid))-oxytocin, a highly potent analogue of oxytocin not bound by neurophysin. *Biochem. J.* 1971; **125**: 909–911.
74. Mouillac B, Chini B, Balestre MN, Elands J, Trumpp KS, Hoflack J, Hibert M, Jard S, Barberis C. The binding site of neuropeptide vasopressin V1a receptor. Evidence for a major localization within transmembrane regions. *J. Biol. Chem.* 1995; **270**: 25 771–25 777.
75. Sawyer WH, Manning M. Synthetic analogs of oxytocin and the vasopressins. *Annu. Rev. Pharmacol.* 1973; **13**: 1–17.
76. Kimura T, Makino Y, Saji F, Takemura M, Inoue T, Kikuchi T, Kubota Y, Azuma C, Nobunaga T, Tokugawa Y. Molecular characterization of a cloned human oxytocin receptor. *Eur. J. Endocrinol.* 1994; **131**: 385–390.
77. Fanelli F, Barbier P, Zanchetta D, De Benedetti PG, Chini B. Activation mechanism of human oxytocin receptor: a combined study of experimental and computer-simulated mutagenesis. *Mol. Pharmacol.* 1999; **56**: 214–225.
78. Williams PD, Bock MG, Evans BE, Freidinger RM, Pettibone DJ. Progress in the development of oxytocin antagonists for use in preterm labor. *Adv. Exp. Med. Biol.* 1998; **449**: 473–479.